Reduction of turbulent fluctuations and crossphase through driven sheared flow on the Large Plasma Device

D.A. Schaffner,[1] T.A Carter,[1] G.D. Rossi,[1] D.S. Guice,[1] J. Maggs,[1] S. Vincena,[1] and B. Friedman[1]
Department of Physics and Astronomy, University of Los Angeles.

(Dated: 6 February 2012)

The effect of flow and flow shear on plasma turbulence has long been studied as a mechanism for turbulence reduction and increased particle confinement in both tokamaks and linear machines. The most dramatic observed effect of cross-field flow is the creation of a higher confinement state, called an H-mode, which has been first observed on the Continuous Current Tokamak (CCT) and in other tokamaks such as DII-D. While some plasma machines rely on a spontaneous flow to create sheared flow for study, other machines (TEXTOR, LAPD) have developed external biasing mechanisms to produce radial electric fields which can drive controllable azimuthal flow by $E \times B$ drift on many machines including TEXTOR[1].

Theoretical investigation into the nature of effect of sheared flow has focused mainly on its influence on turbulent fluctuations[5] and on the crossphase between electric field and any advected quantity, such as density in the case of particle flux[6,7]. Fluctuation reduction due to shear comes from the reduction in radial correlation length—due to the shearing of turbulent eddies—while the effect of crossphase has to do with the fact that turbulent particle flux relies on the phasing of outward or inward ExB flows with increases in density. The simplest mode non-specific models for the effect of shearing on turbulent fluctuations predict a power law decrease[5], while crossphase can have an even stronger scaling[7].

The experiment in this letter is an extension of previous biasing experiments on LAPD. In one, an inward pointing electric field produced by chamber biasing demonstrated that increased flow shear resulted in turbulent modification and increased particle confinement[2]. However, penetration of the electric field was low until high biases resulting in sudden transition from background states to confined states. In another experiment, it was shown that a small biased annulus could produce sheared flows within the main column of the plasma[3]. In this letter, a new biasing mechanism has allowed for smooth transition from a low flow shear state-LAPD's natural state-to zero shear state, to a high shear state. With this smooth control of flow shear, we can carefully observe the effect of shear on turbulent fluctuations, particle flux, and gradient length scale to a level of detail that allows for comparison to theory prediction.

In this letter, we report on the observation of a degraded and enhanced confinement state as a function of driven sheared-flows and that this confinement occurs regardless of flow or flow shear direction. We have shown that this variation in confinement correlates with increases and decreases in particle flux. Moreover, we can show that radial correlation length, particle flux, crossphase, density fluctuations and floating potential fluctions all decrease with shearing rate, and can each be fit to a power-law decay as predicted by theory. Lastly, we note that the various quantities effect by shearing are modified differently dependent on what frequency regime they are examimned.

The Large Plasma Device[4] (LAPD) is a 20m by 1m cylindrical linear device with a 54cm wide barium-oxide coated nickel cathode pulsed at 1Hz to produce a 45eV electron beam which ionizes the helium gas in the chamber. A column long plasma of density about 5×10^{12} cm^3 and temperature of 5eV is produced. The field for this experiment was set to 1000G. To produce the bias, four quarter annulus aluminum plates are inserted half a meter beyond the cathode creating a flat boundary condition from the chamber wall to the opening of a 25cm aperture. A pulse power circuit connected to a capacitor bank supplies a 5ms bias during the 15ms plasma discharge with a voltage range from floating potential to 230V. Measurements of saturated current and floating potential are taken with a 9-tip flush surface tantalum probe while temperature and plasma potential is taken by swept Langmuir probe.

Azimuthal flow and flow shear are controlled by adjusting the voltage on the capacitor bank which produces a voltage on the limiter places. When voltages of the limiter on are approximately less than the voltage of the anode (between floating potential of about 35V to about 45V with respect to chamber ground), an overall azimuthal flow occurs in the ion diamagnetic direction shown in Fig. 1with velocities peaking just outside the limiter edge. When the voltage on the limiter is brought near anode potential, flow and flow shear zero out. Voltages above anode produce electron diamagnetic direction flows peaked at the limiter edge. The voltage on the power supply cannot be set below the floating potential as the plasma tends to charge the capacitor banks.

Measurements of saturated current and particle flux are taken for each bias flow state. A set of radial values are averaged over a range from 27 to 31cm in a region where such averaged flow and flow shear scale approximately linearly with limiter bias as in Fig. 2and are outside the limiter edge to avoid any possible effects from fast electrons.

Calculated quantites are used to characterize flux and length scale. Density gradient length scale is calculated by $L_\xi = |\nabla \ln \xi|^{-1}$ while particle flux, $\Gamma_p = \langle \tilde{n}\tilde{v_r} \rangle =$

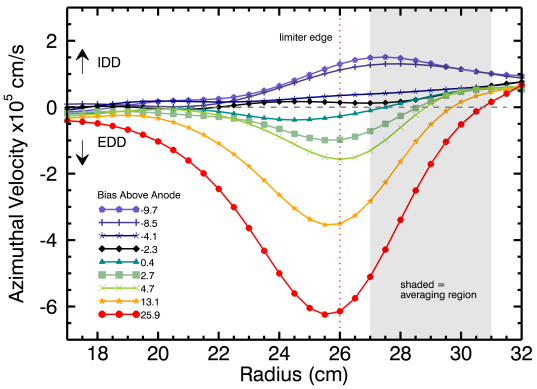

FIG. 1. Velocity profiles using plasma potential from swept measurements.

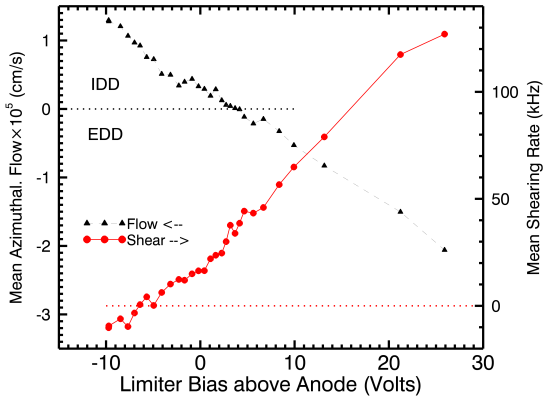

FIG. 2. Nearly linear scaling of flow (black) and shearing (red) versus limiter bias.

$\langle \tilde{n}\tilde{E}_\theta \rangle / B$, can be calculated spectrally as

$$\Gamma_p = \frac{2}{B}\int_0^\infty |n(\omega)||E_\theta(\omega)|\gamma_{n,E_\theta}(\omega)\cos[\phi_{n,E_\theta}(\omega)]d\omega. \quad (1)$$

which also allows us to directly determine the contributions of turublent fluctuations, crossphase and coherency to the particle flux.

This letter presents the first detailed experimental investigation into the effect of shearing rate variation on particle flux, turbulent fluctuations and crossphase through a wide range of shearing rates. The ability to have both a no flow, no shear regime and sheared to strongly sheared regimes in both azimuthal directions allows us to begin comparing experimental data to the proposed theoretical predictions. Furthermore, the no flow, no shear regime allows us to directly measure a turbulent decorrelation rate. An autocorrelation time of about

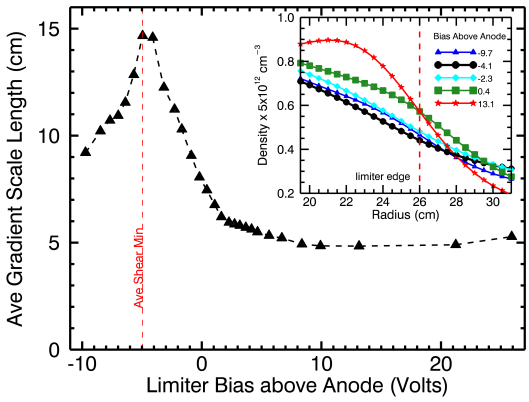

FIG. 3. Density gradient length scale versus limiter bias. Inset shows density profile relaxing then steepening again with bias.

36us is calculated by taking the full width at half max of a Hilbert transform of the isat autocorrelation function at the no flow/shear bias yielding a decorrelation rate of about $\Delta\omega_t = 28$kHz. The first clear observation shown in Fig. 3 is a change in particle confinement level as bias is varied, as indicated by a change in the gradient scale length of the density radial profiles. The average density gradient scale length begins at 9cm with no bias, but as the limiter voltage increase to the point of minimum shearing rate, the density gradient levels out, reaching a scale length peak of about 15cm. As bias and shearing continue to increase, the density gradient steepens again fairly symmetrical about the shear minimum. Pushing the voltage higher causes the density gradient to steepen further reaching a saturated value of about 5cm. The initial scale length value and saturated values are consistent with previous biasing experiments done on the LAPD, but rather than see a density gradient degradation, a sharp threshold is observed. It is likely the new biasing setup allows this transition to be observed.

It should be noted that the symmetry of the gradient scale length curve about the shear minimum is an indication that both IDD or EDD flow and shearing direction can produce a steepened density gradient. This is clearly seen in Fig. 4 with average gradient scale length compared to the ratio of shearing rate to decorrelation rate. Both IDD and EDD flow and flow shear points lie on the same curve.

The changes in gradient scale length are indicative of an overall change in particle flux. This flux can be directly measured by correlating fluctuating density with fluctuating radial flow—$E \times B$ flow using an electric field derived from two floating potential tips on either side of the density measuring saturated current tip. This flux can be rewritten in terms of an integral over fluctuation power, coherency and crossphase allowing separate

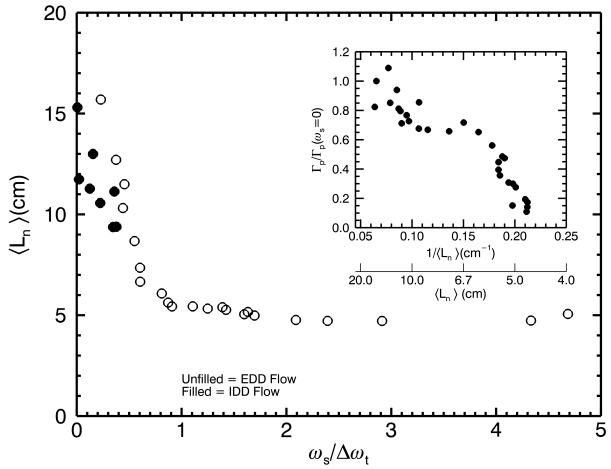

FIG. 4. Gradient scale length versus shearing rate. Inset shows correlation of gradient scale length and shearing rate.

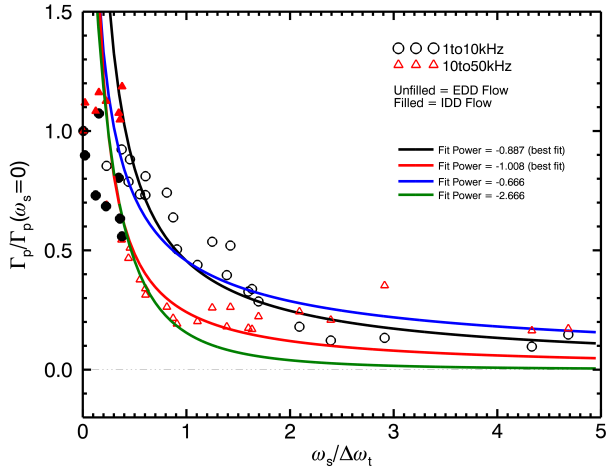

FIG. 5. Particle flux as a function of shearing rate normalized to decorrelation rate. Black points show low frequency, red shows high. Filled symbols represent points with flow in IDD.

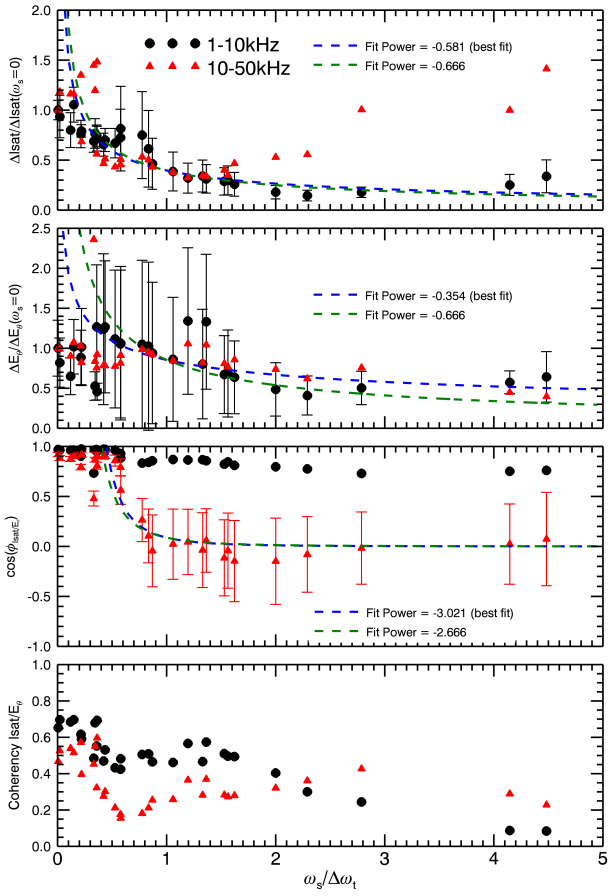

FIG. 6. Components of particle flux versus shearing rate including isat/Density fluctuation power(a), electric field fluctuation power(b), crossphase(c) and coherency(d) with black points for low frequency, red for high.

comparison of the effect of shearing on turbulent power or crossphase. In addition to separating the contributions of fluctuation power and crossphase to the flux, the flux can be calculated over a certain frequency range. Like gradient scale length, normalized average particle flux decreases with shearing rate scaled to the turbulent decorrelation rate as in Fig. 5. However, a clear difference emerges when the flux is bandwidth limited. The flux from 1 to 10kHz, where most of the fluctuation power is located, drops off gradually, hitting its minimum only at a shearing rate about three times the decorrelation rate. Higher bandwidth though, 10 to 50kHz, drops off much more quickly, nearing its minimum when shearing equals decorrelation rate. Best fit lines to log-log plots of these scatters give power decay exponents of about $-2/3$ for the low bandwidth flux and about $-8/3$ for the high bandwidth flux.

The reason for the difference becomes evident when the flux is examined by its separate components as in Fig. 6 . The top two plots show fluctuations power, saturated current and electric field, as functions of normalized shearing rate, while the bottom two show crossphase and coherency respectively. Observing the low bandwidth flux, both isat power and E-field power decrease gradually, with power fits on the order of $-2/3$. Crossphase, on the other hand, does not decrease. In this bandwidth then, decreases in flux are primarily due to decreasing turbulent power. For high bandwidth flux, though, the opposite appears to be true. While isat fluctuations do decrease initially, they actually begin to increase at high shearing rates. Electric field fluctuations, meanwhile, do not appear to change much with shearing. In this case, decrease in flux is primarily due to drops in crossphase and to some extent coherency. Power fits to this high frequency crossphase calculation are about $-8/3$. Both fits for fluctuation power and for crossphase are consistent with predicted values and trends from theory.

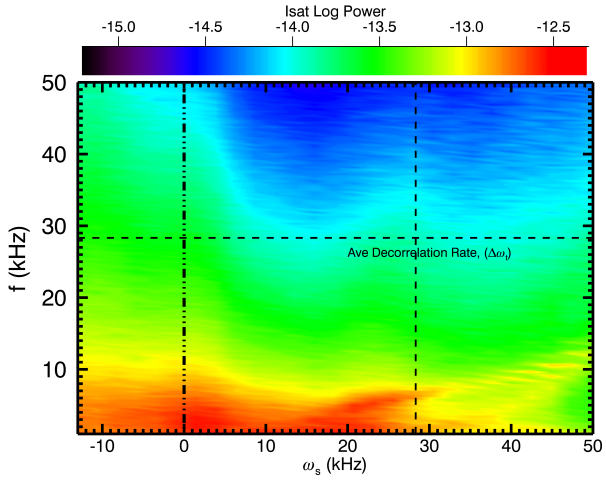

FIG. 7. Contour plot of log isat fluctuation power versus shearing rate and frequency. Dashed lines show location of decorrelation rate.

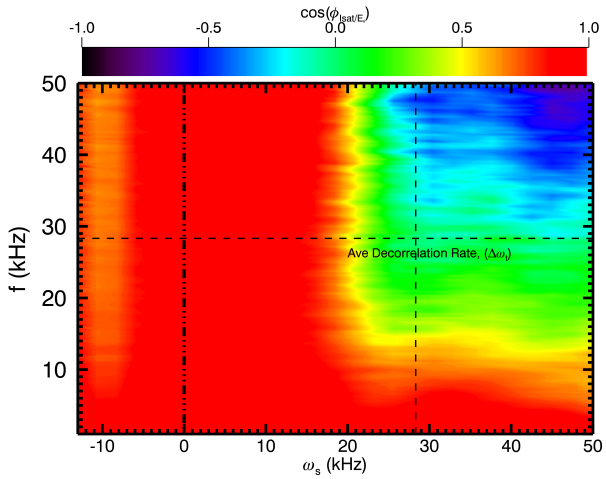

FIG. 8. Contour plot isat/E-field crossphase versus shearing rate and frequency. Dashed lines show location of decorrelation rate.

The frequency dependence on flux is even more evident in Fig. 7 showing a contour map of fluctuation power or crossphase versus frequency and shearing rate. Isat power peaks at zero shearing rate and tends to decrease gradually for all frequencies up to about 20kHz. Crossphase however Fig. 8 , shows no change from unity for all frequencies below 10kHz, but the exhibits sharp drops from 10kHz and above, starting consistently at about 20kHz.

From these results, it is clear that both decreases in turbulent fluctuations and crossphase can lead to a decrease in radial particle flux, and consequently, a steepening of density gradients—i.e. confinement. However, both processes appear to be most effective in different regimes. Fluctuations decreases seem to manifest in lower shearing rate, lower frequencies while crossphase change is most apparent at higher shearing rate and higher frequencies. The reason for this difference is still under examination, but could be a result of a relationship between of turbulent correlation length and shearing scale length or perhaps due to the growth of new instabilities associated with flow and shearing including Kelvin-Helmholtz or rotational interchange modes. Evidence for this last point exists in the isat fluctuation power of Fig. 7 where a coherent mode appears in the low frequency range at high shearing rate as well as the fact that high frequency isat fluctuations actually increase with shearing rate. Whether this mode is connected to the effect of shearing on flux or just a separate consequence of driving up the shearing and flow is unclear.

This letter presents the first detailed scan of shearing rate in a linear device and has shown a clear effect of particle flux and density confinement through both the mechanisms of turbulent fluctuation reduction and change in crossphase of saturated current and electric field. Moreover, the scan has allowed for comparison to theory predictions of the effect of shearing on both fluctuation power and crossphase. Fits of the data for both fluctuations and crossphase are consistent with the power law predictions proposed.

[1] J. Boedo, D. Gray, S. Jachmich, R. Conn, G. Terry, G. Tynan, G. V. Oost, R. Weynants, and T. Team, Nucl. Fusion **40**, 7 (2000).
[2] T. Carter and J. Maggs, Phys. Plasmas **16**, 012304 (2009).
[3] S. Zhou, W. Heidbrink, H. Boehmer, R. McWilliams, T. Carter, S. Vincena, B. Friedman, and D. Schaffner, Phys. Plasmas **19**, 99999999 (2012).
[4] W. Gekelman, H. Pfister, Z. Lucky, J. Bamber, D. Leneman, and J. Maggs, Rev. Sci. Instrum. **62**, 2875 (1991).
[5] H. Biglari, P. Diamond, and P. W. Terry, Phys. Fluids B. **2**, 1–4 (1990).
[6] A. Ware, P. Terry, P. Diamond, and B. Carreras, Plasma Phys. Control Fusion **38**, 1343–1347 (1996).
[7] P. Terry, D. Newman, and A. Ware, Phys. Rev. Lett. **87**, 18 (2001).